BEILSTEIN JOURNAL OF ORGANIC CHEMISTRY

Supporting Information

for

Substituent effect on TADF properties of 2-modified 4,6-bis(3,6-di-*tert*-butyl-9-carbazolyl)-5-methylpyrimidines

Irina Fiodorova, Tomas Serevičius, Rokas Skaisgiris, Saulius Juršėnas
and Sigitas Tumkevicius

Beilstein J. Org. Chem. **2022,** *18,* 497–507. doi:10.3762/bjoc.18.52

Copies of NMR spectra and extended photophysical properties

Table of contents

Copies of ^{1}H and ^{13}C NMR, and HRMS spectra

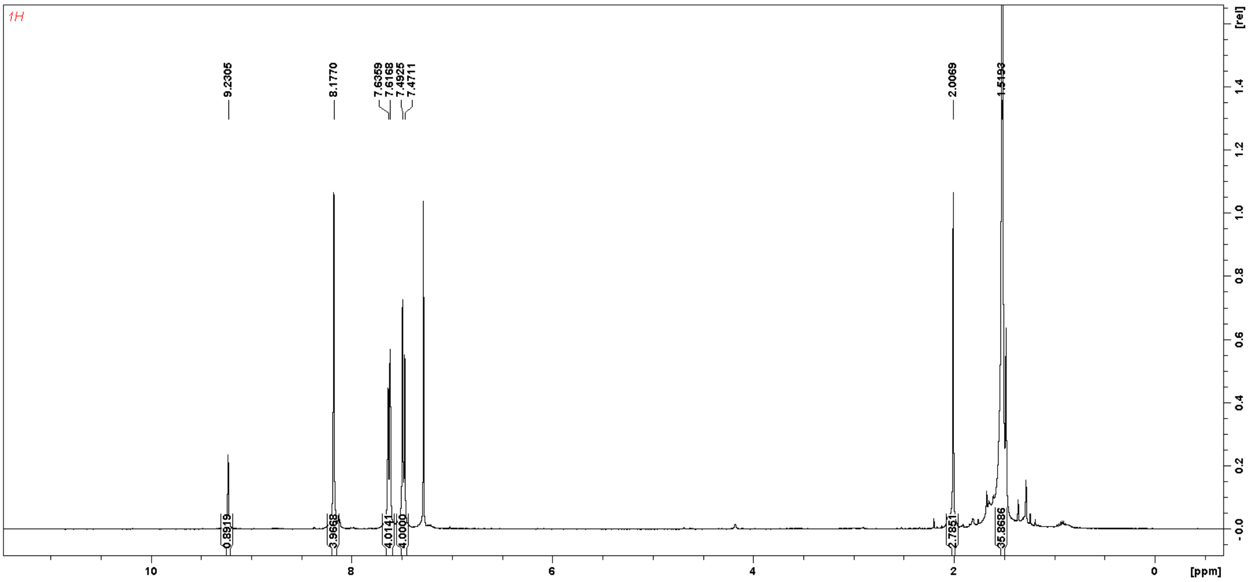

Figure S1. ^{1}H NMR spectrum of 4,6-bis[3,6-di(*tert*-butyl)-9*H*-carbazol-9-yl]-5-methylpyrimidine (**1**).

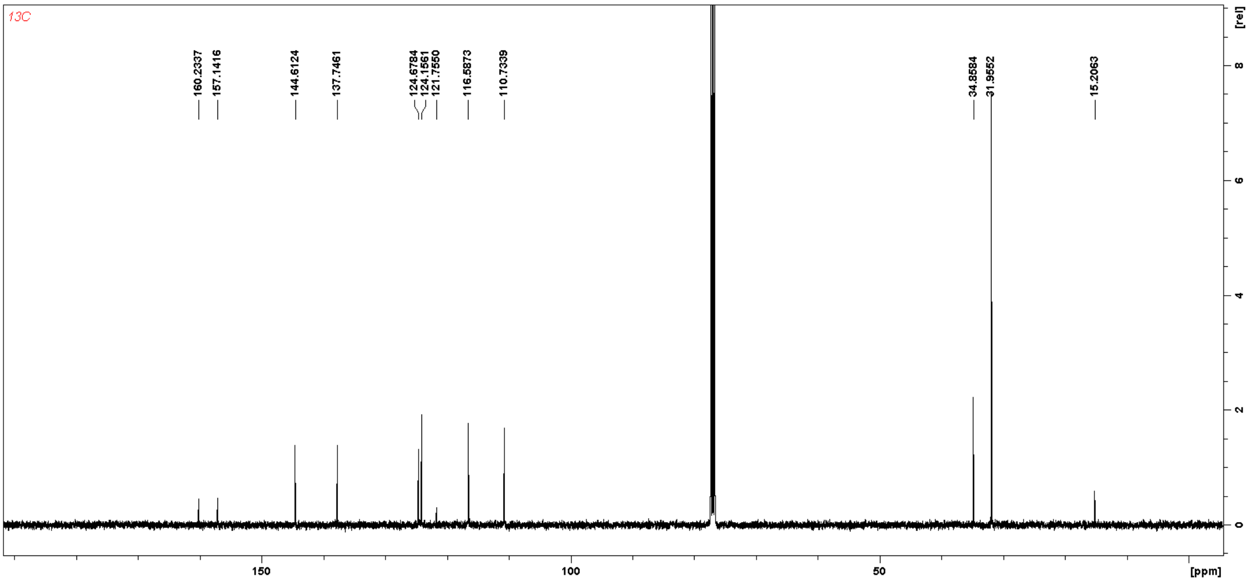

Figure S2. ^{13}C NMR spectrum of 4,6-bis[3,6-di(*tert*-butyl)-9*H*-carbazol-9-yl]-5-methylpyrimidine (**1**).

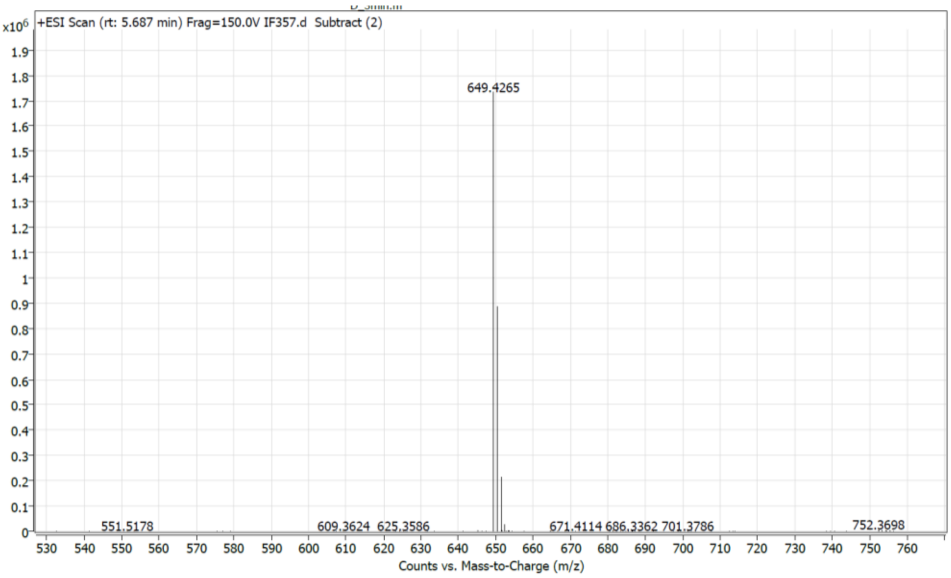

Figure S3. HRMS spectrum of 4,6-bis[3,6-di(*tert*-butyl)-9*H*-carbazol-9-yl]-5-methylpyrimidine (**1**).

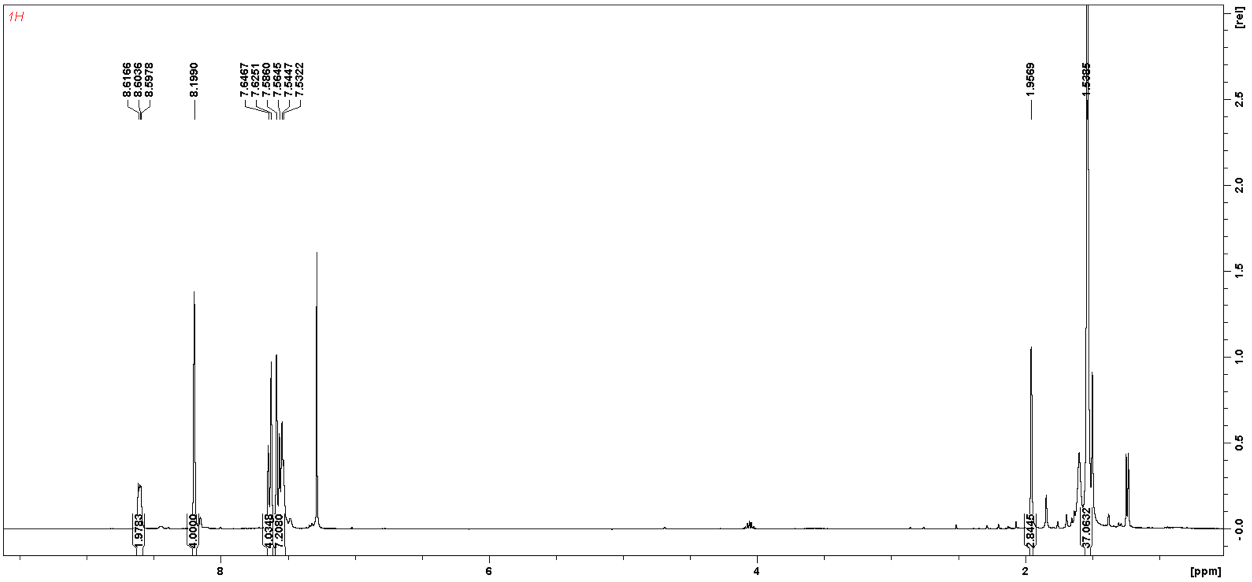

Figure S4. ^{1}H NMR spectrum of 4,6-bis[3,6-di(*tert*-butyl)-9*H*-carbazol-9-yl]-5-methyl-2-phenylpyrimidine (**2a**).

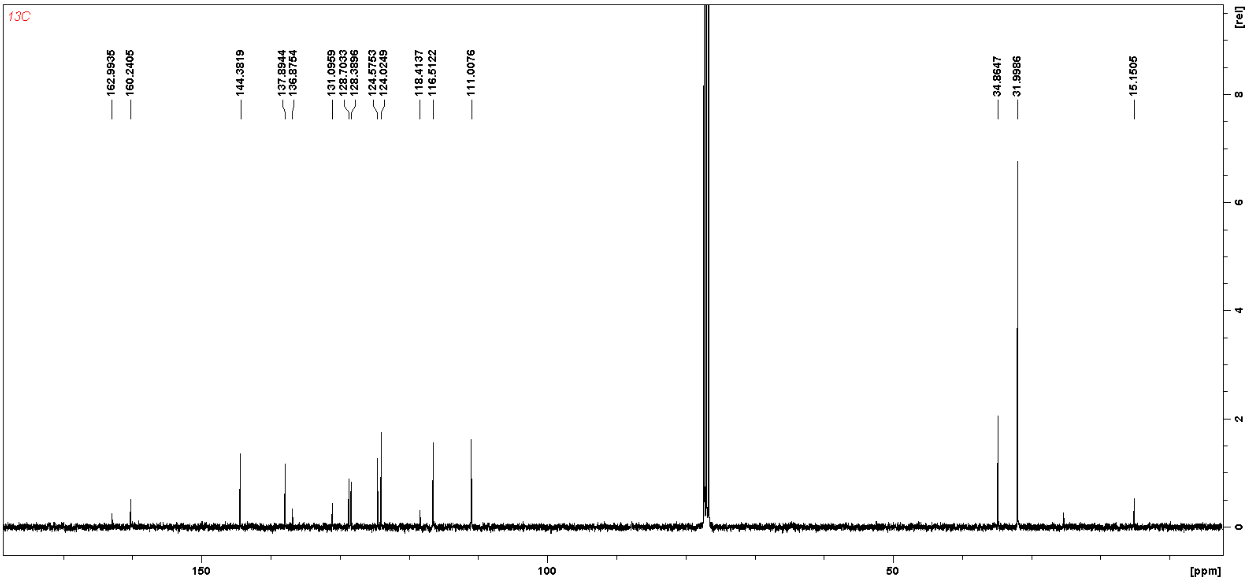

Figure S5.^{3}C NMR spectrum of 4,6-bis[3,6-di(*tert*-butyl)-9*H*-carbazol-9-yl]-5-methyl-2-phenylpyrimidine (**2a**).

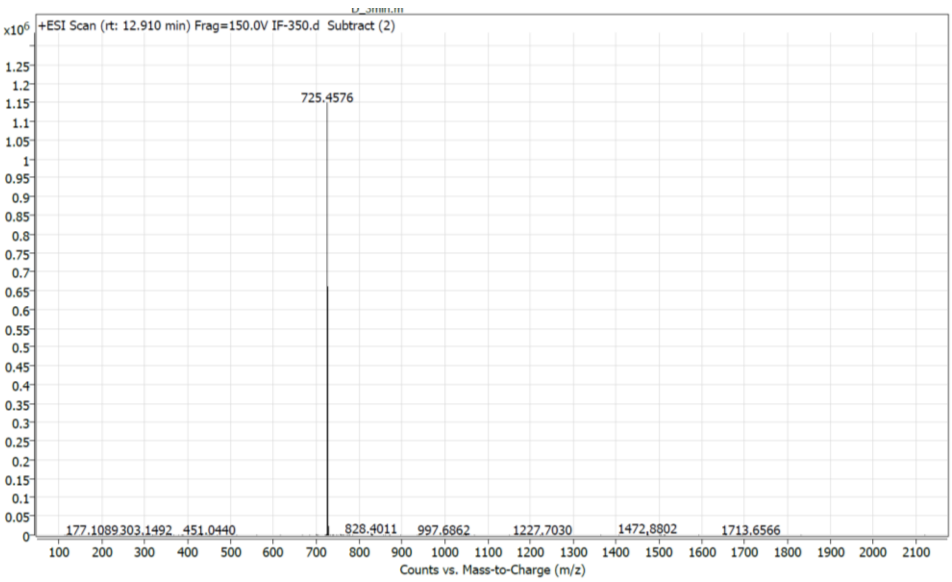

Figure S6. HRMS spectrum of 4,6-bis[3,6-di(*tert*-butyl)-9*H*-carbazol-9-yl]-5-methyl-2-phenylpyrimidine (**2a**).

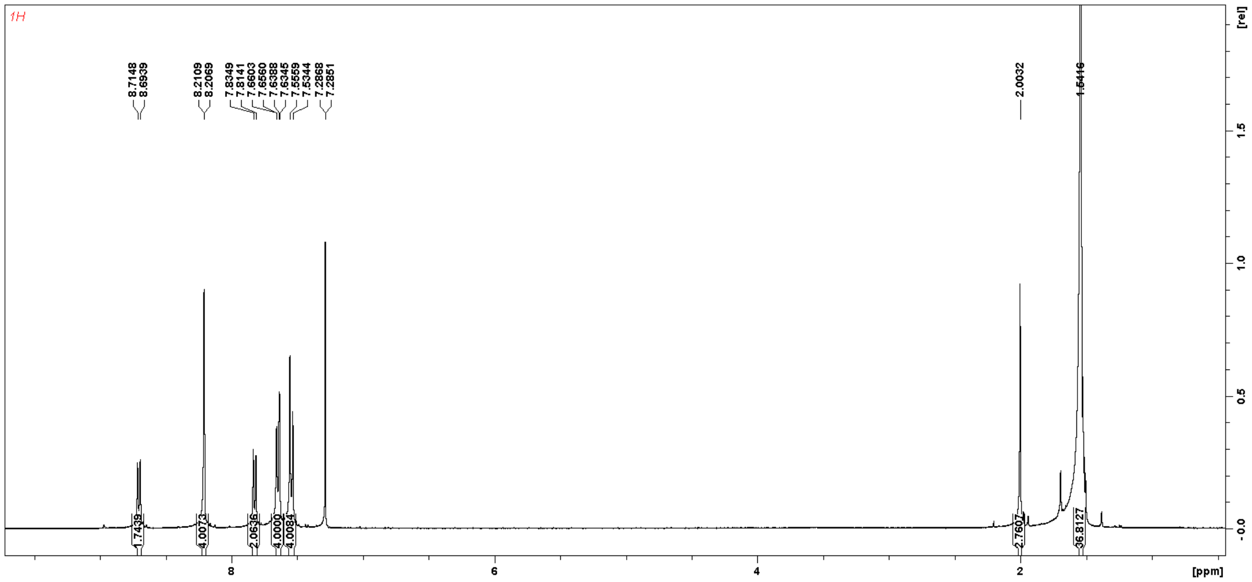

Figure S7. ^{1}H NMR spectrum of 4,6-bis[3,6-di(*tert*-butyl)-9*H*-carbazol-9-yl]-2-(4-cyanophenyl)-5-methylpyrimidine (**2b**).

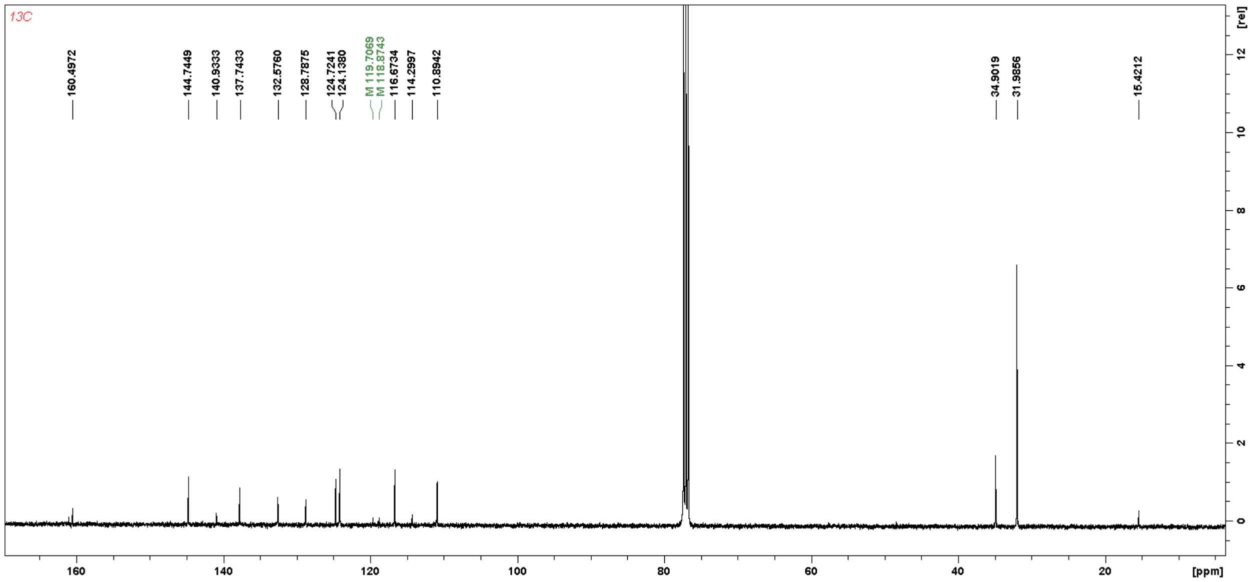

Figure S8. ^{13}C NMR spectrum of 4,6-bis[3,6-di(*tert*-butyl)-9*H*-carbazol-9-yl]-2-(4-cyanophenyl)-5-methylpyrimidine (**2b**).

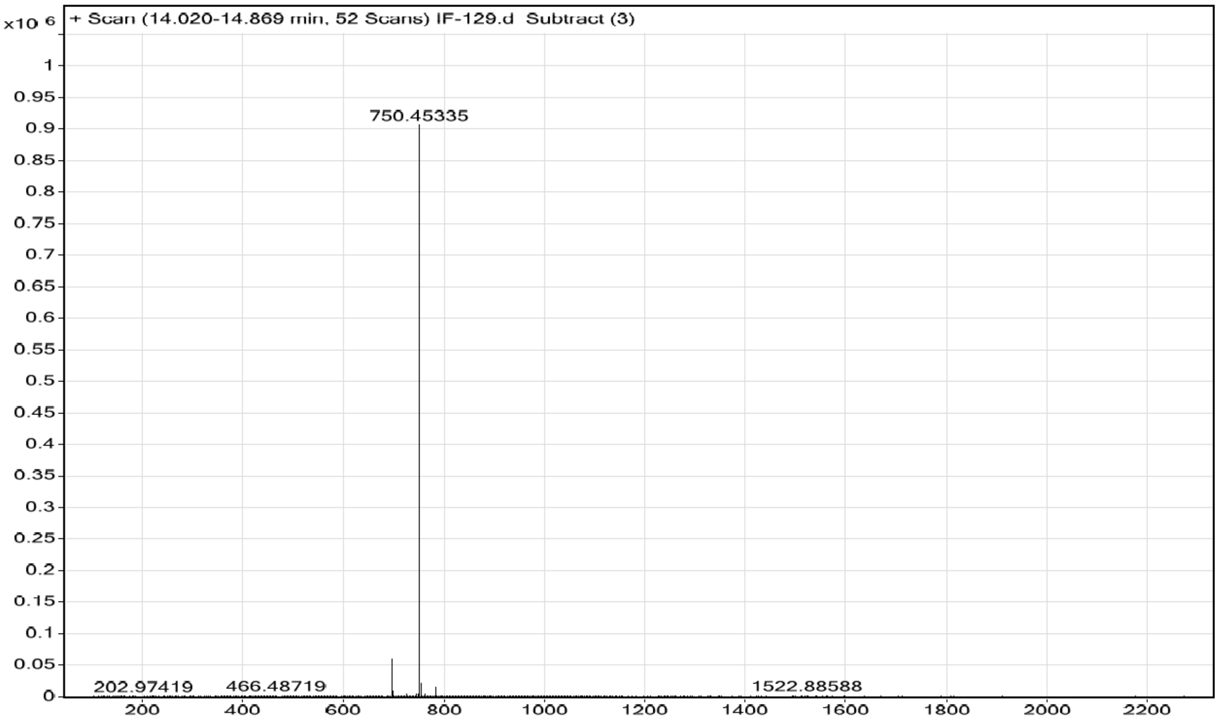

Figure S9. HRMS spectrum of 4,6-bis[3,6-di(*tert*-butyl)-9*H*-carbazol-9-yl]-2-(4-cyanophenyl)-5-methylpyrimidine (**2b**).

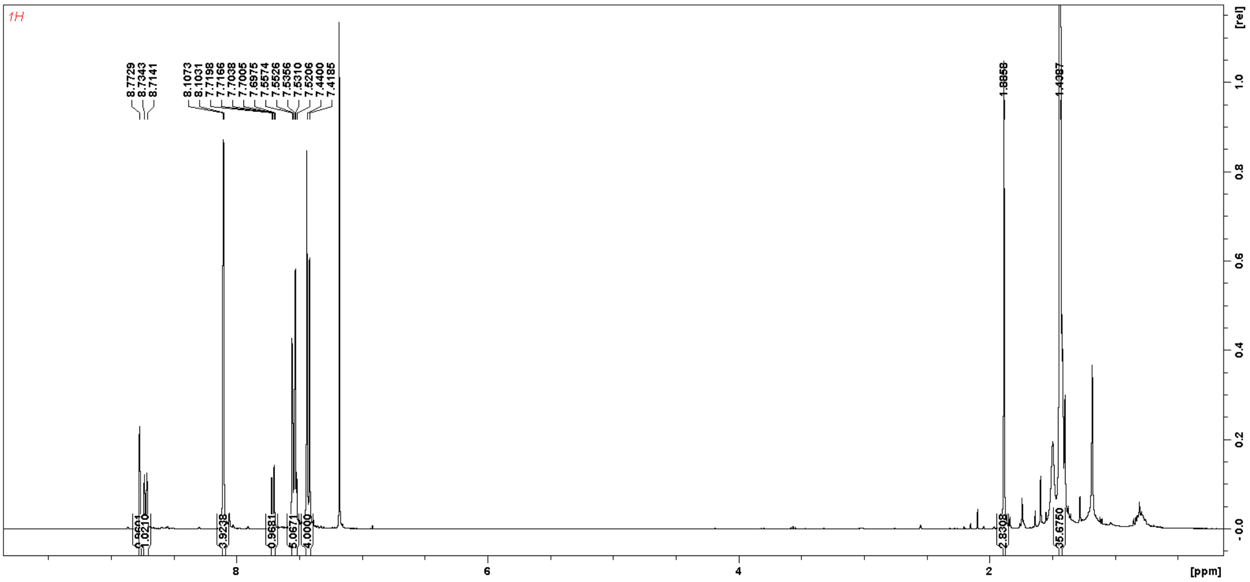

Figure S10. ^{1}H NMR spectrum of 4,6-bis[3,6-di(*tert*-butyl)-9*H*-carbazol-9-yl]-2-(3-cyanophenyl)-5-methylpyrimidine (**2c**).

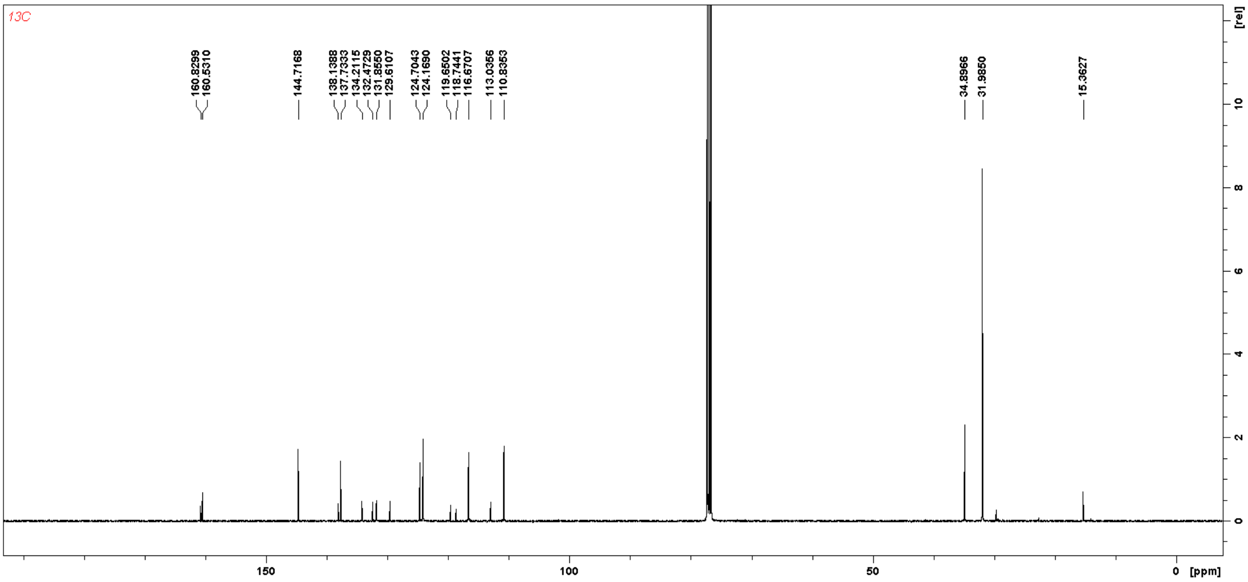

Figure S11. ^{13}C NMR spectrum of 4,6-bis[3,6-di(*tert*-butyl)-9*H*-carbazol-9-yl]-2-(3-cyanophenyl)-5-methylpyrimidine (**2c**).

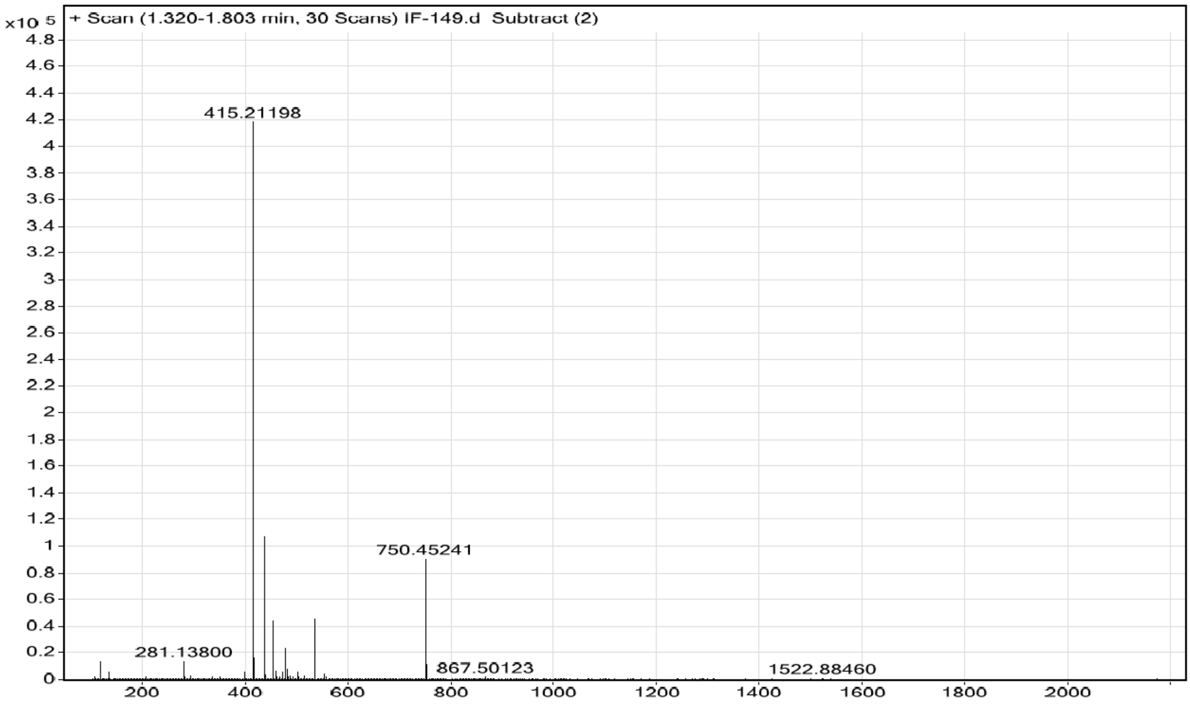

Figure S12. HRMS spectrum of 4,6-bis[3,6-di(*tert*-butyl)-9*H*-carbazol-9-yl]-2-(3-cyanophenyl)-5-methylpyrimidine (**2c**).

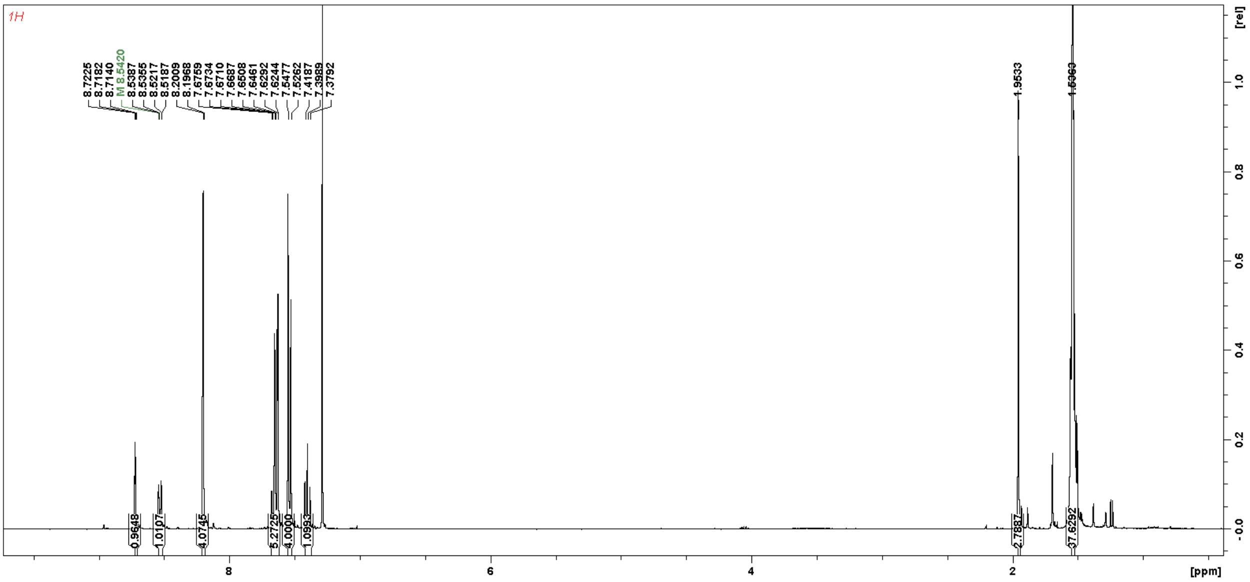

Figure S13. ^{1}H NMR spectrum of 4,6-bis[3,6-di(*tert*-butyl)-9*H*-carbazol-9-yl]-2-(3-bromophenyl)-5-methylpyrimidine (**2d**).

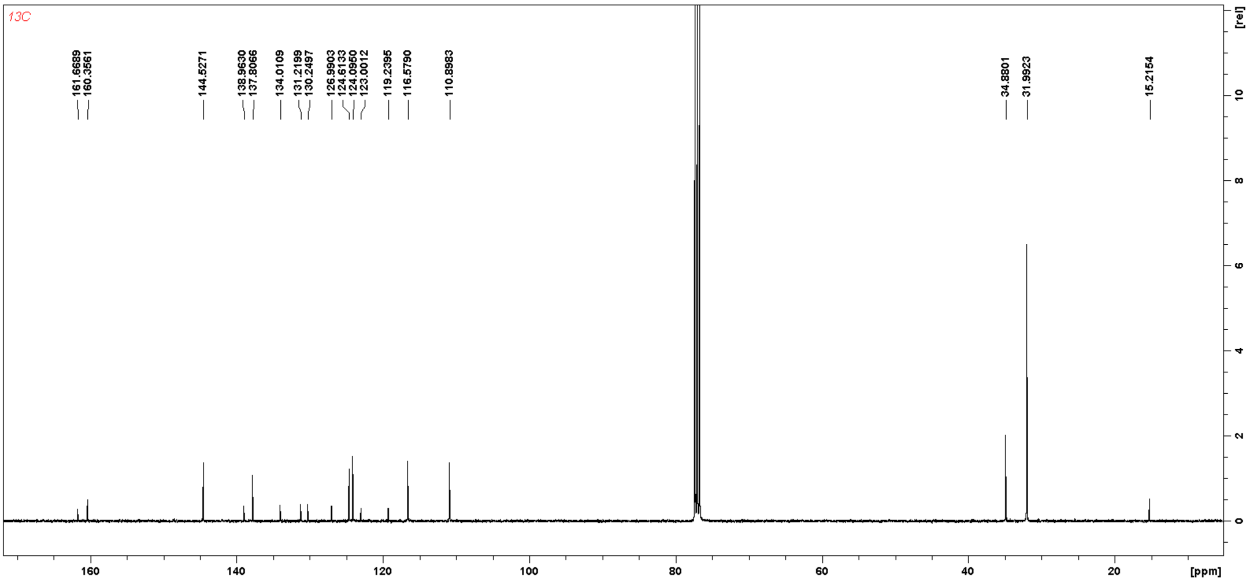

Figure S14. ^{13}C NMR spectrum of 4,6-bis[3,6-di(*tert*-butyl)-9*H*-carbazol-9-yl]-2-(3-bromophenyl)-5-methylpyrimidine (**2d**).

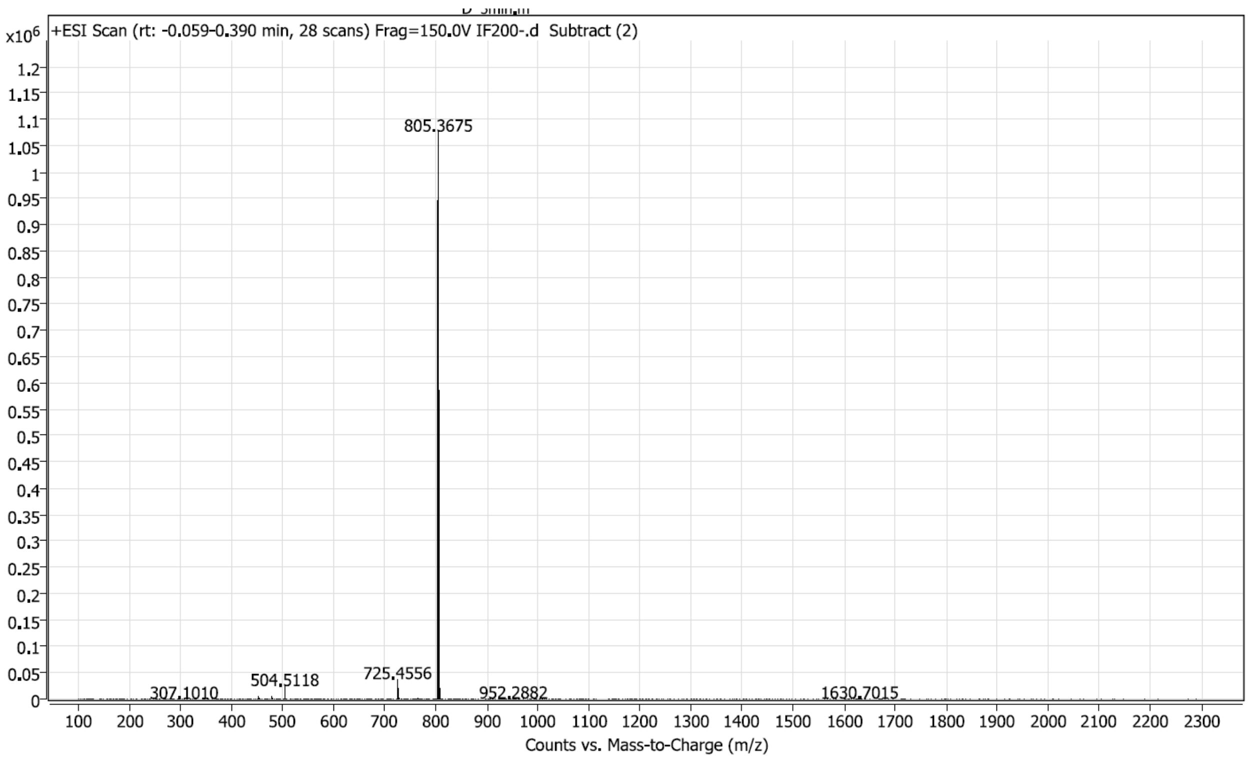

Figure S15. HRMS spectrum of 4,6-bis[3,6-di(*tert*-butyl)-9*H*-carbazol-9-yl]-2-(3-bromophenyl)-5-methylpyrimidine (**2d**).

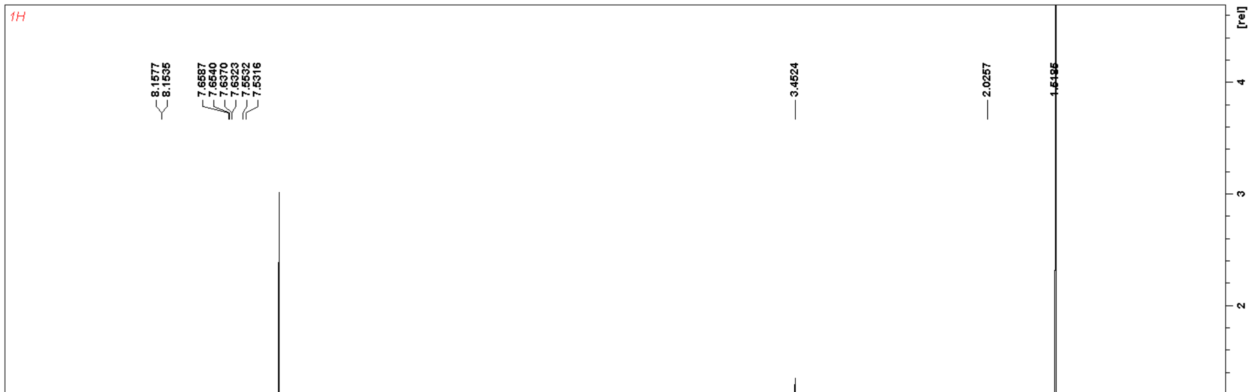

Figure S16. ^{1}H NMR spectrum of 4,6-bis(3,6-di-*tert*-butyl-9*H*-carbazol-9-yl)-5-methyl-2-methylsulfonylpyrimidine (**3**).

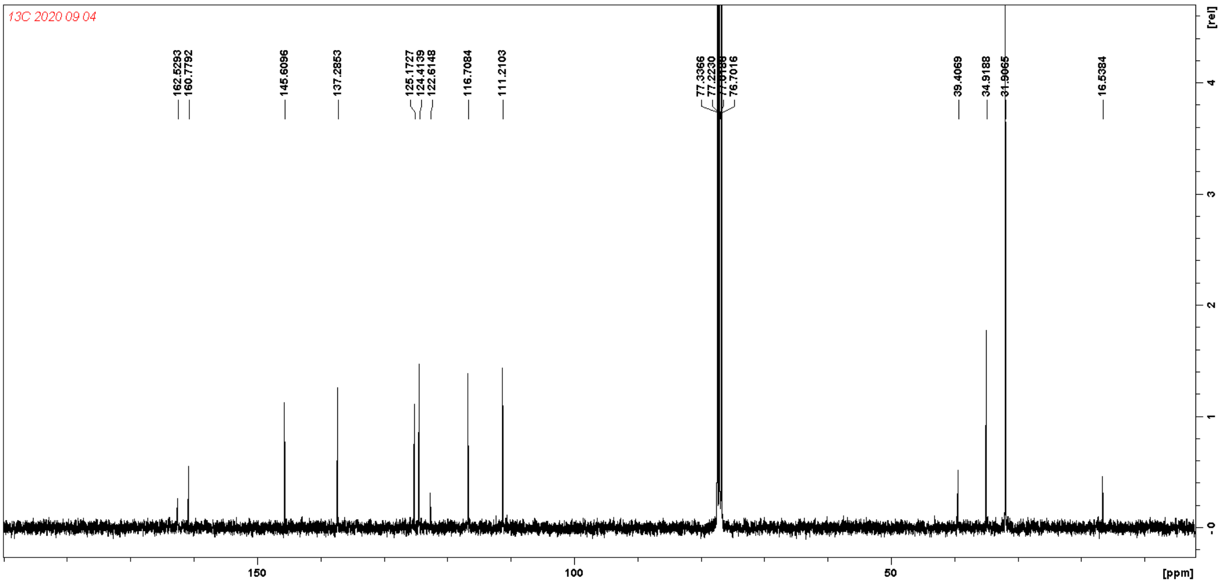

Figure S17. ^{13}C NMR spectrum of 4,6-bis(3,6-di-*tert*-butyl-9*H*-carbazol-9-yl)-5-methyl-2-methylsulfonylpyrimidine (**3**).

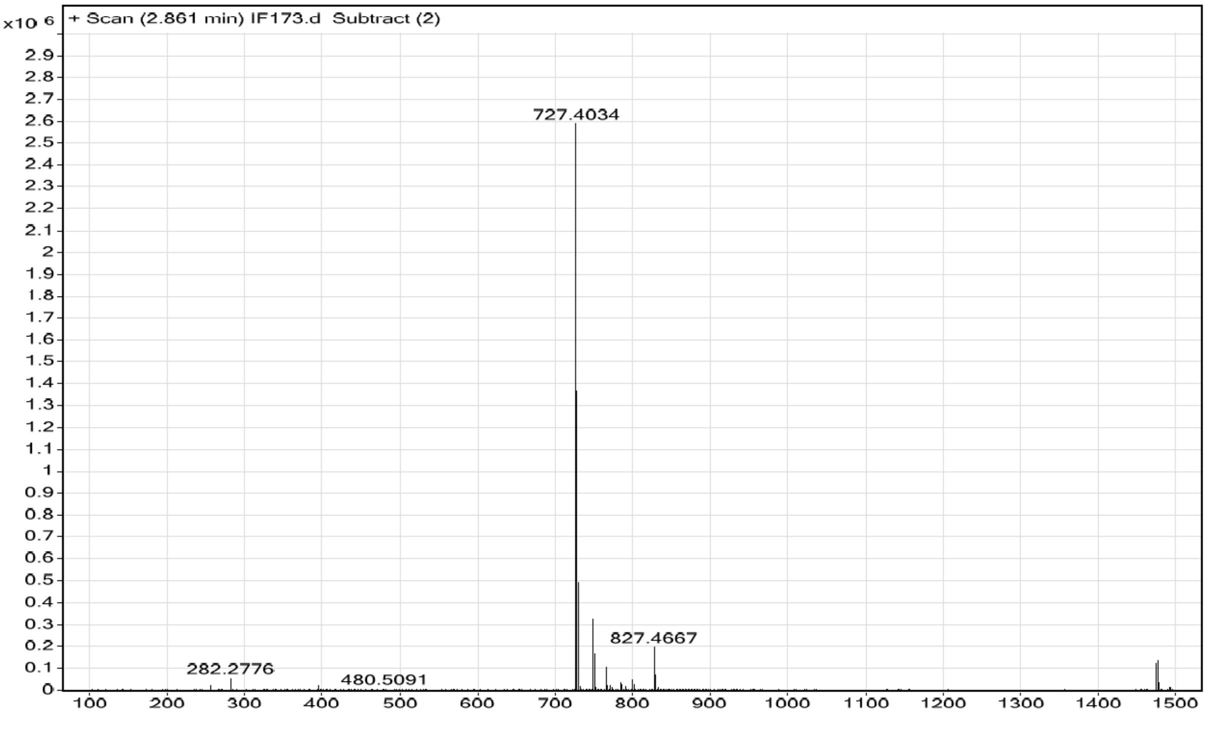

Figure S18. HRMS spectrum of 4,6-bis(3,6-di-*tert*-butyl-9*H*-carbazol-9-yl)-5-methyl-2-methylsulfonylpyrimidine (**3**).

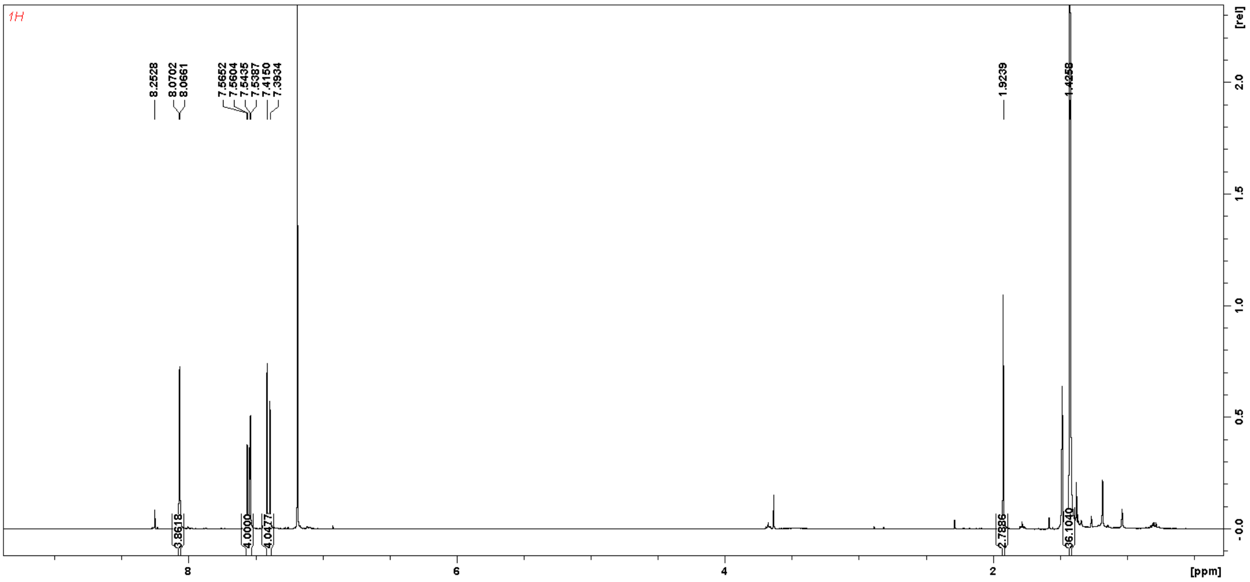

Figure S19. ^{1}H NMR spectrum of 4,6-bis(3,6-di-*tert*-butyl-9*H*-carbazol-9-yl)-5-methylpyrimidine-2-carbonitrile (**4**).

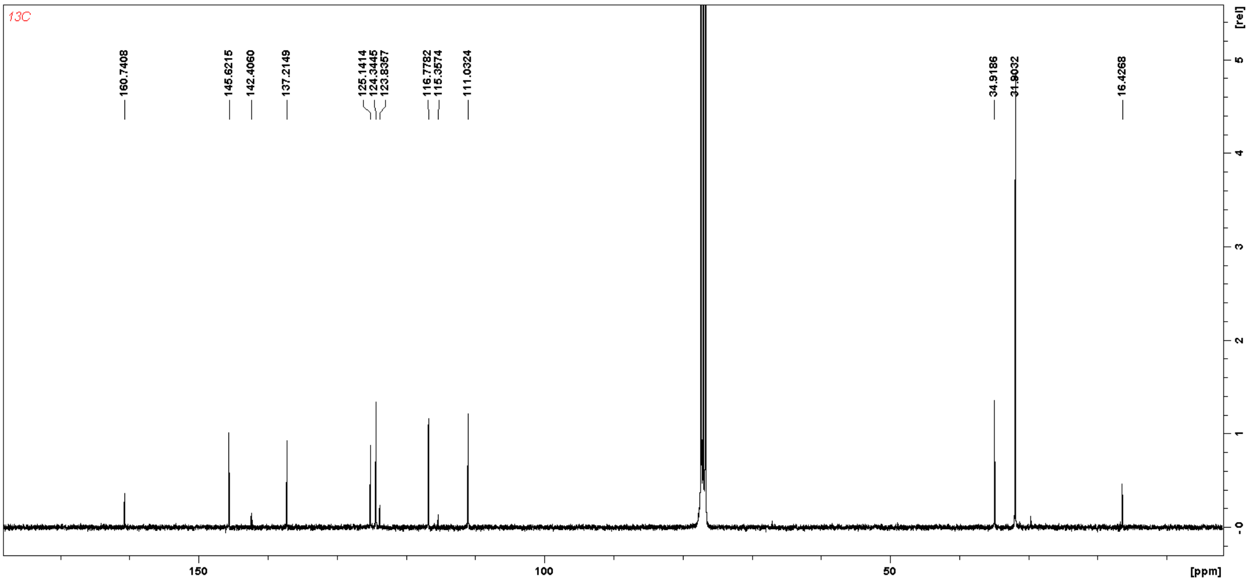

Figure S20. ^{13}C NMR spectrum of 4,6-bis(3,6-di-*tert*-butyl-9*H*-carbazol-9-yl)-5-methylpyrimidine-2-carbonitrile (**4**).

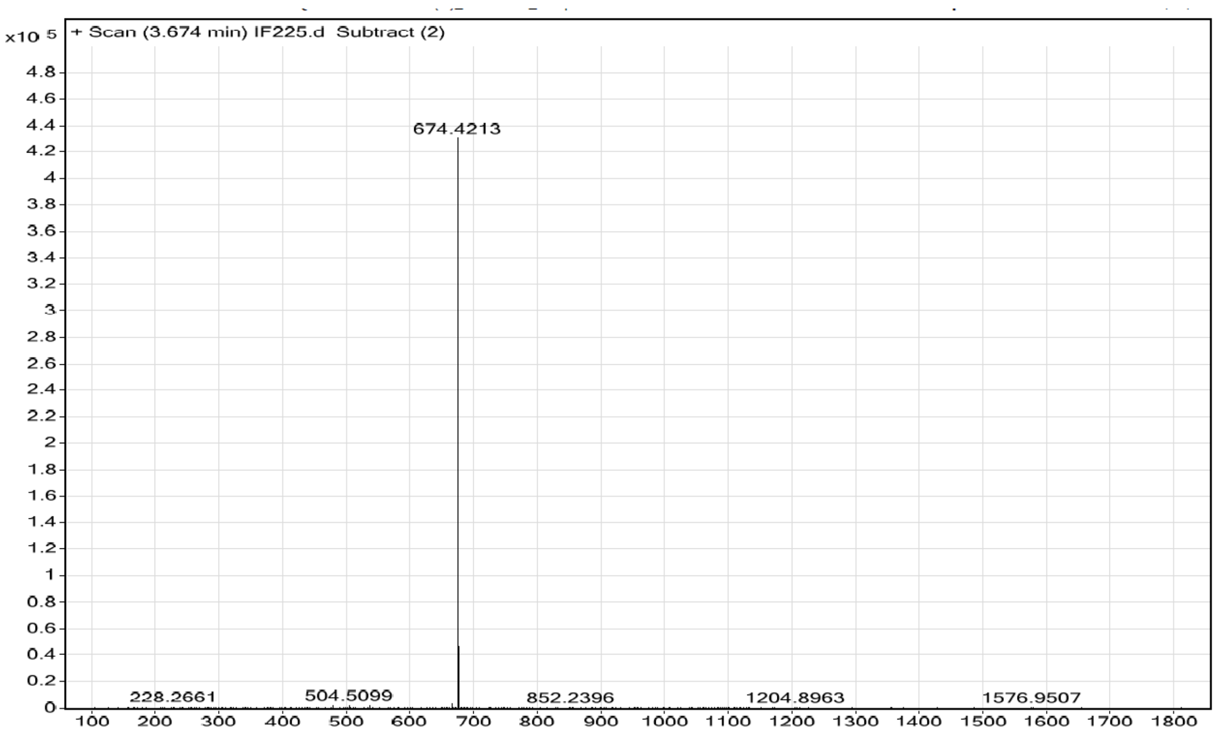

Figure S21. HRMS spectrum of 4,6-bis(3,6-di-*tert*-butyl-9*H*-carbazol-9-yl)-5-methylpyrimidine-2-carbonitrile (**4**).

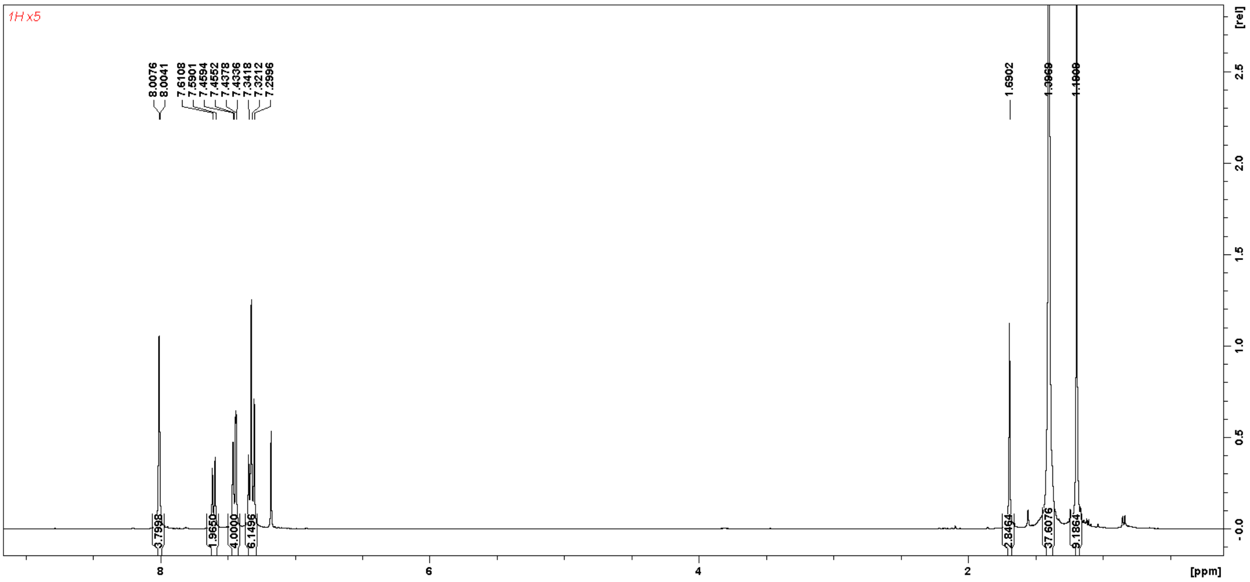

Figure S22. ^{1}H NMR spectrum of 4,6-bis[3,6-di(*tert*-butyl)-9*H*-carbazol-9-yl]-2-[4-(*tert*-butyl)phenylthio]-5-methylpyrimidine (**5**).

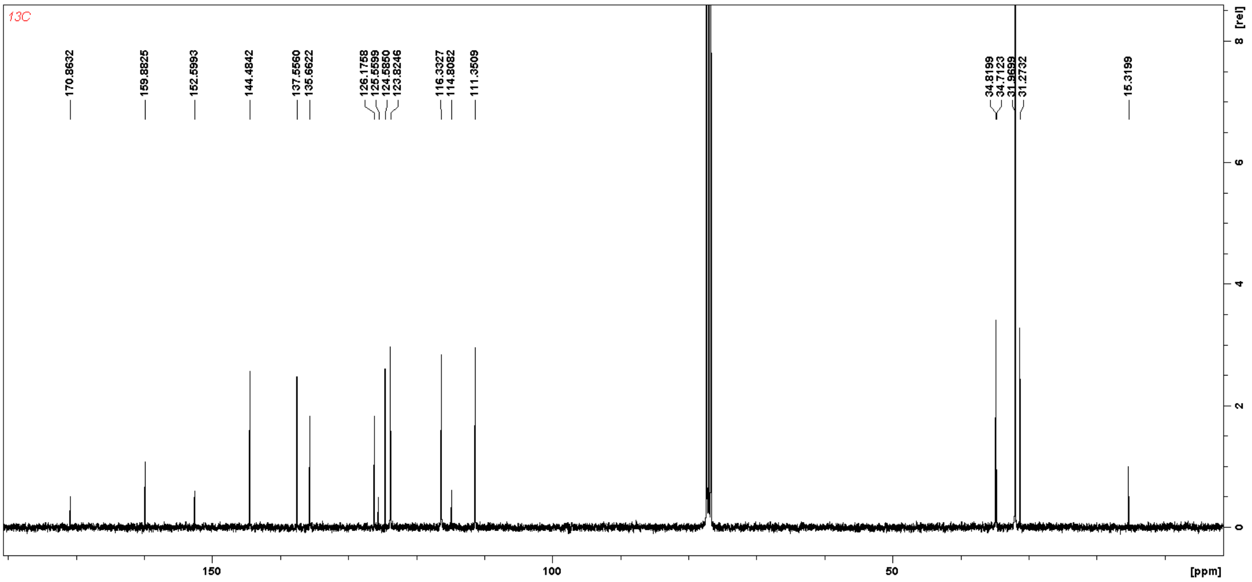

Figure S23. ^{13}C NMR spectrum of 4,6-bis[3,6-di(*tert*-butyl)-9*H*-carbazol-9-yl]-2-[4-(*tert*-butyl)phenylthio]-5-methylpyrimidine (**5**).

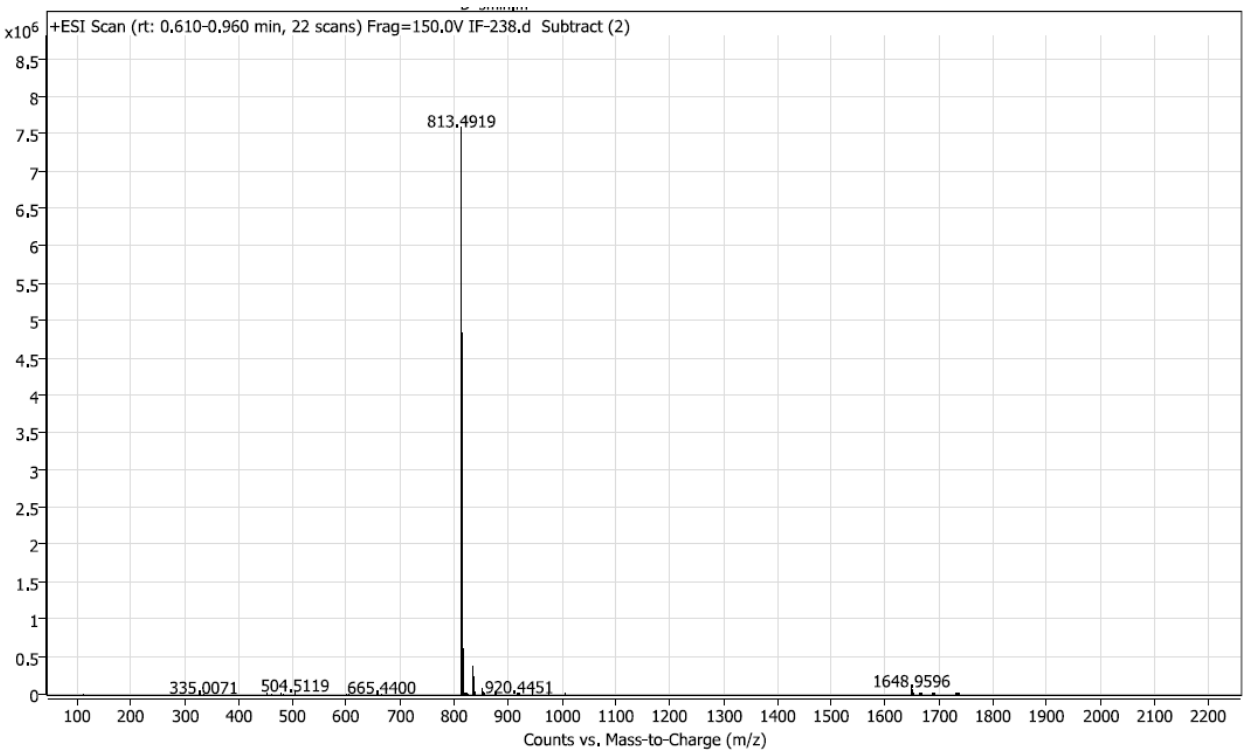

Figure S24. HRMS spectrum of 4,6-bis[3,6-di(*tert*-butyl)-9*H*-carbazol-9-yl]-2-[4-(*tert*-butyl)phenylthio]-5-methylpyrimidine (**5**).

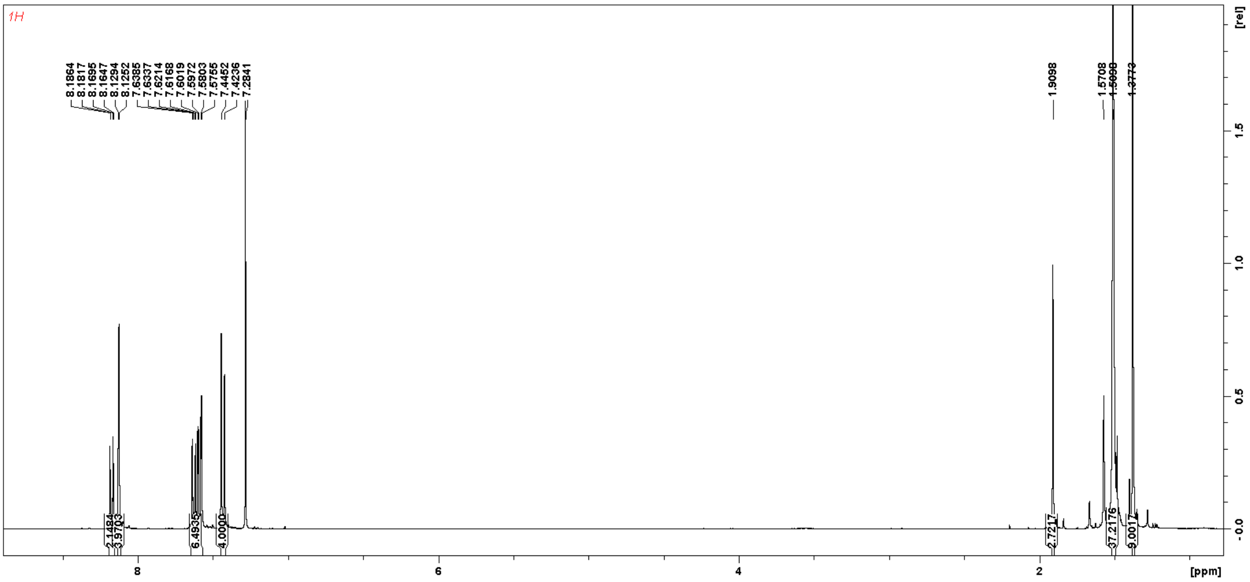

Figure S25. ^{1}H NMR spectrum of 4,6-bis[3,6-di(*tert*-butyl)-9*H*-carbazol-9-yl]-2-[4-(*tert*-butyl)phenylsulfonyl]-5-methylpyrimidine (**6**).

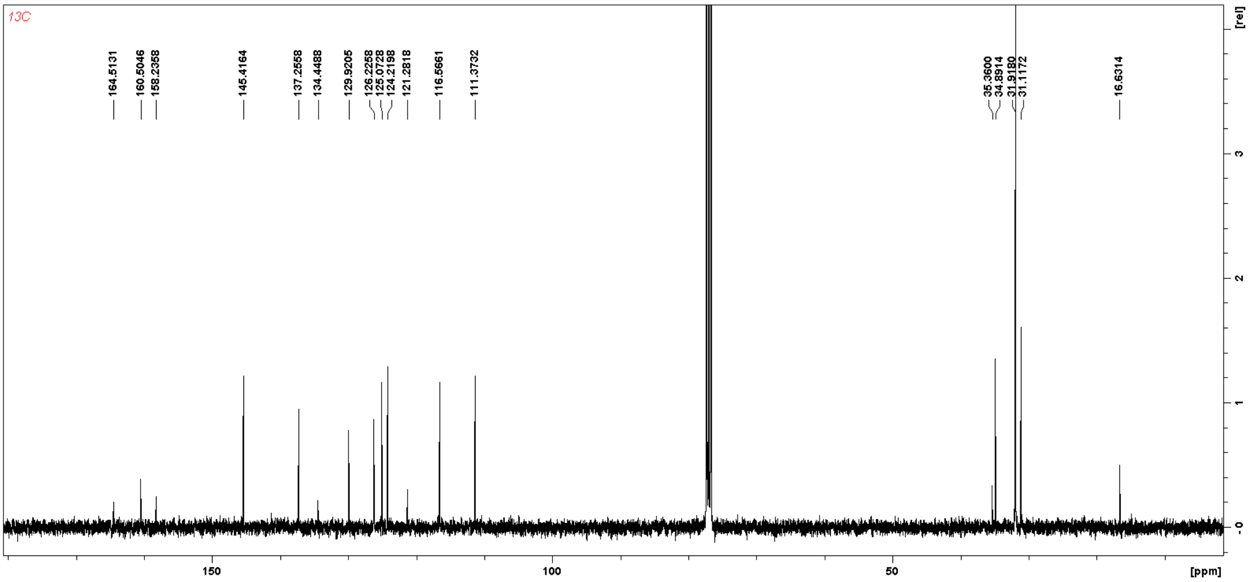

Figure S26. ^{13}C NMR spectrum of 4,6-bis[3,6-di(*tert*-butyl)-9*H*-carbazol-9-yl]-2-[4-(*tert*-butyl)phenylsulfonyl]-5-methylpyrimidine (**6**).

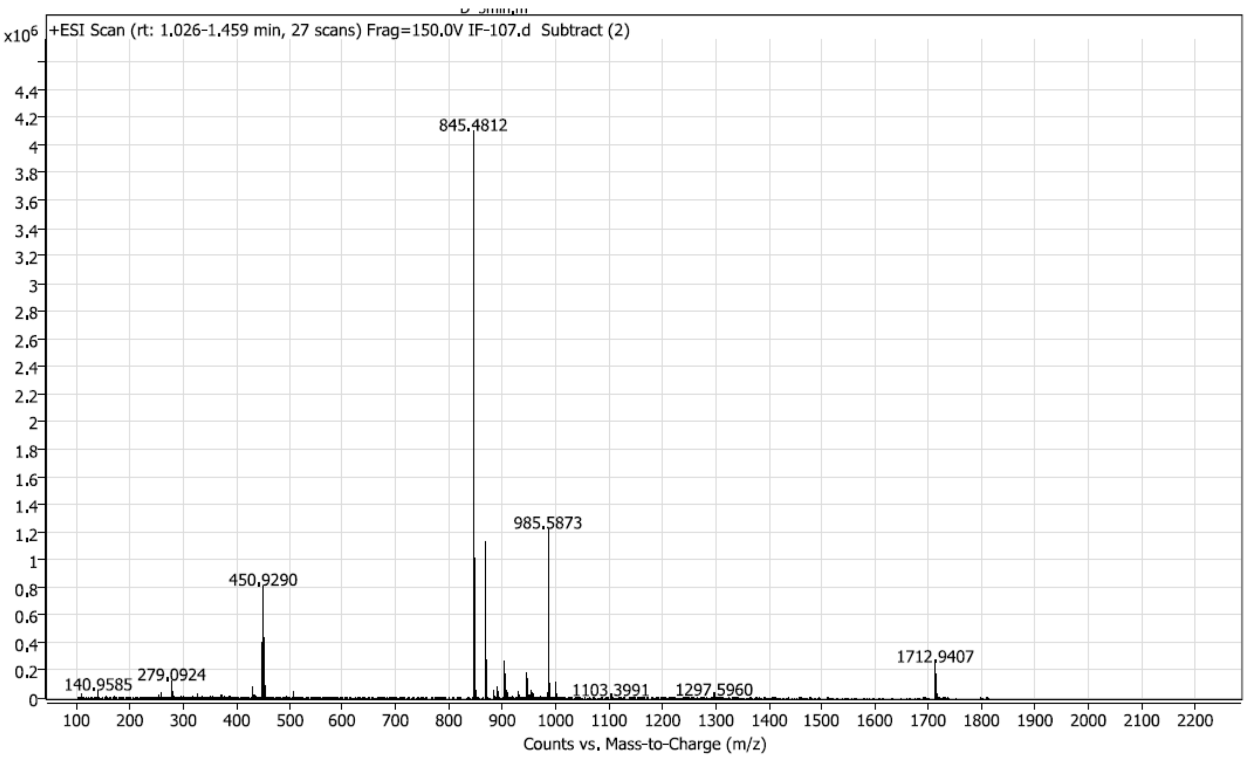

Figure S27. HRMS spectrum of 4,6-bis[3,6-di(*tert*-butyl)-9*H*-carbazol-9-yl]-2-[4-(*tert*-butyl)phenylsulfonyl]-5-methylpyrimidine (**6**).

Extended photophysical properties

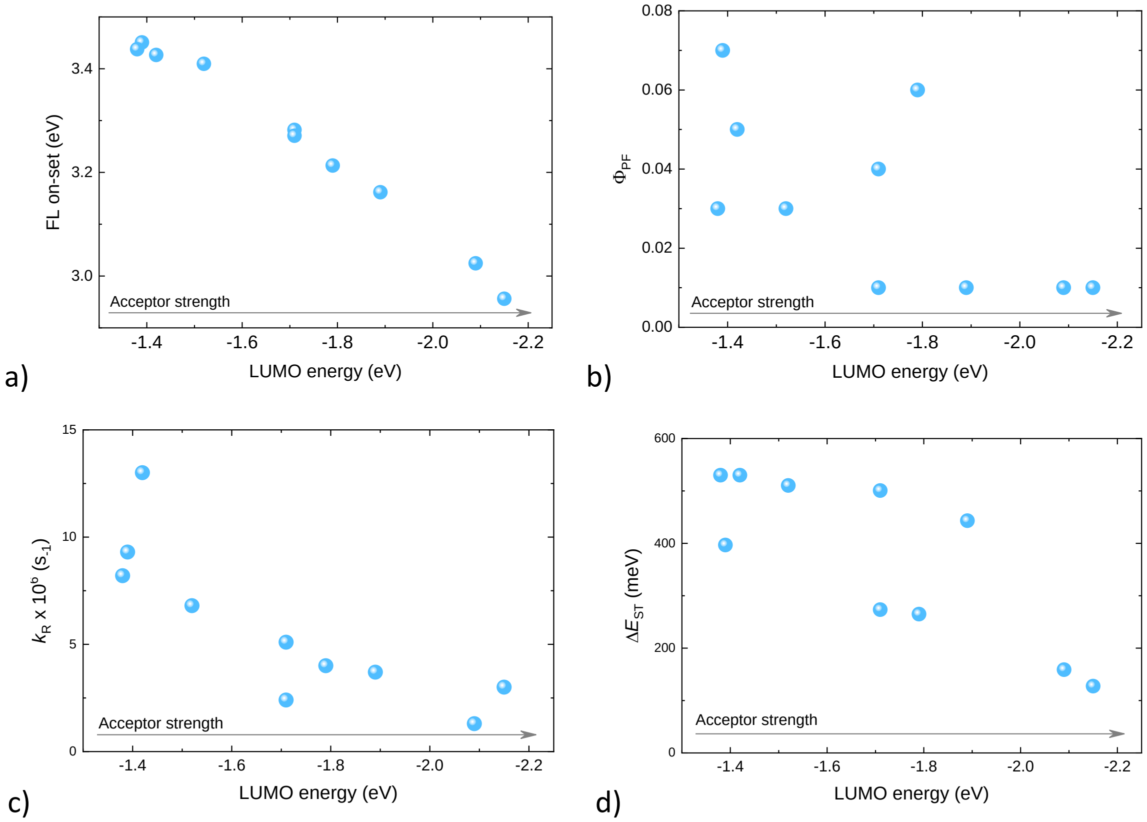

Figure S28. a) Fluorescence on-set energy, b) PF quantum yield, c) k_r and d) ΔE_{ST} as a function of LUMO energy.

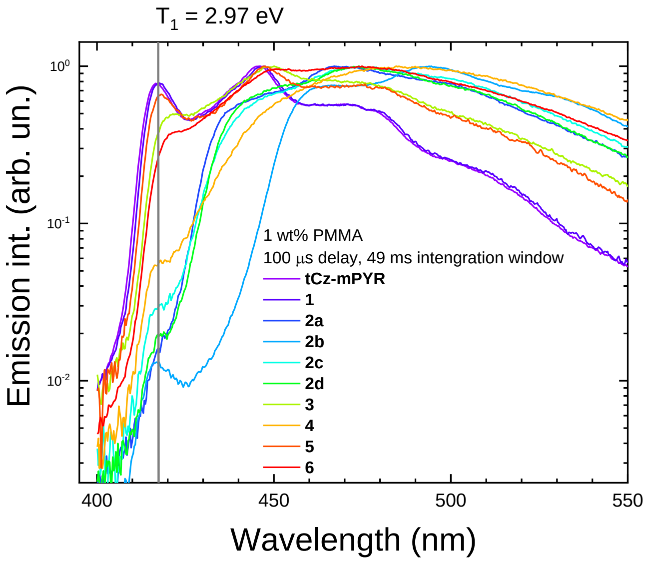

Figure S29. Phosphorescence spectra of carbazole–pyrimidine TADF compounds in semi-logarithmic scale.

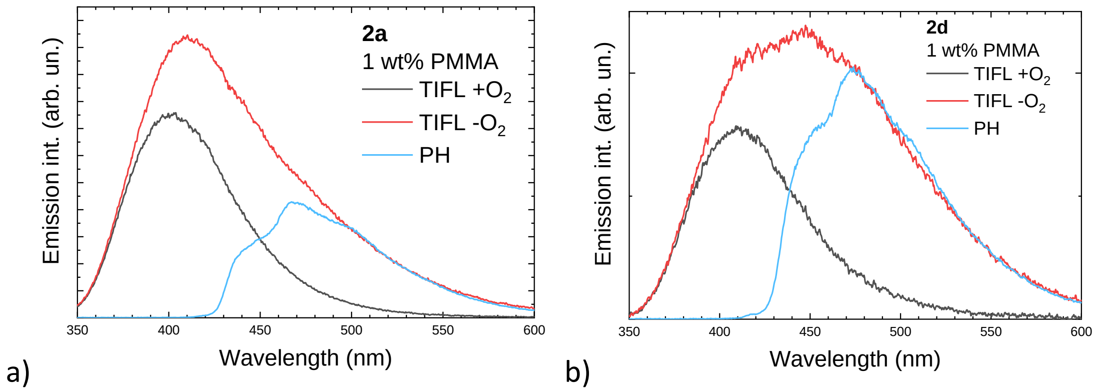

Figure S30. a) TIFL spectra of 1 wt % PMMA films of **2a** in oxygen-saturated (+O₂) and oxygen-free conditions (-O₂) together with PH spectrum at 10 K (intensity of PH spectrum was modified to overlay with low-energy shoulder of TIFL). b) TIFL spectra of 1 wt % PMMA films of **2d** in oxygen-saturated (+O₂) and oxygen-free conditions (-O₂) together with PH spectrum at 10 K (intensity of PH spectrum was modified to overlay with low-energy shoulder of TIFL).

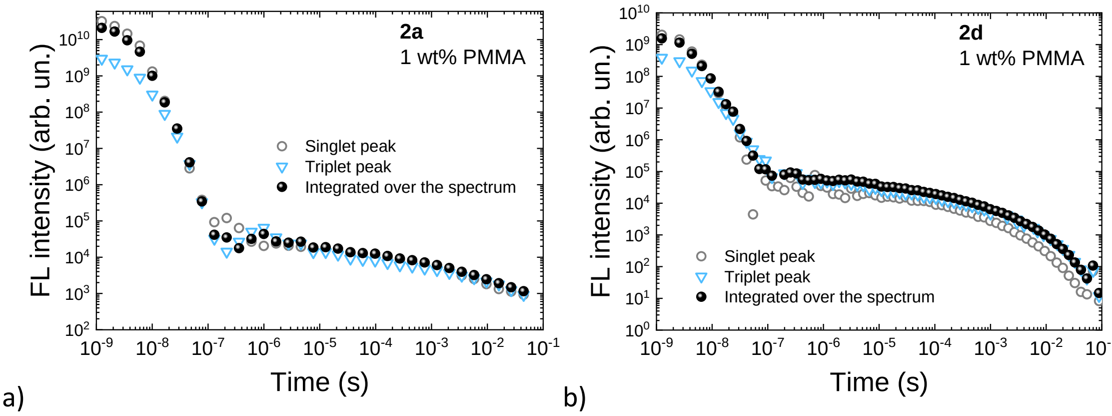

Figure S31. Fluorescence decay transients of 1 wt % PMMA films of **2a** and **2d** in oxygen-free conditions. Grey figures are transients at singlet emission peak, blue figures are transients at triplet emission peak and black figures are the sum of both decays.